Experimental Torsional Vibration Analysis of Different Propellers on a Lycoming O-360 Engine

Jérémie Buiatti, Habib Setti, Himaé Guigne, Yoann Cossec, Samuel Dupland

January 9, 2026

Abstract

This study presents an experimental investigation of torsional vibratory torque in a direct-drive engine–propeller assembly using several propeller configurations. Measurements were performed on a Lycoming O-360-A1D engine instrumented with internal strain gauges, allowing direct measurement of crankshaft torsional loads during ground and flight tests. Four propeller types were evaluated: an aluminium propeller, a wooden propeller, a five-blade carbon-fiber propeller, and a three-blade carbon-fiber propeller.

Vibratory torque data were analyzed using a rainflow cycle counting method, applied to one-second time windows, in order to extract a conservative envelope of high-frequency cyclic loading as a function of engine speed. The results reveal significant differences in torsional resonance behavior between propeller configurations, including pronounced resonances for aluminium and multi-blade carbon-fiber propellers within or near typical operating RPM ranges.

In contrast, the three-blade carbon-fiber propeller designed using dynamic engine-propeller modeling and evolutionary optimization algorithms exhibits reduced vibratory coupling and significantly lower torsional excitation levels. The influence of torsional resonances on crankshaft accelerations and engine accessories is discussed, along with the benefits of resonance placement and operating range reduction. These findings highlight the importance of integrated dynamic design approaches for improving performance, durability, and vibratory behavior of direct-drive propulsion systems.

Keywords: Torsional vibration; Engine–propeller coupling; Direct-drive aircraft engines; Crankshaft torque measurement; Rainflow cycle counting; Propeller resonance; Vibratory fatigue; Carbon-fiber propellers; Evolutionary optimization; Engine accessories loading

1. Experimental Setup

Torsional vibration measurements were conducted on a direct-drive engine–propeller assembly using the following propeller configurations:

- Aluminium propeller (SENSENICH 76EM8S14-0-60)
- Wooden propeller (HOFFMANN HO 7 HM-180 160)
- Five-blade carbon-fiber propeller : Aluminium hub and blade root, carbon blades (DUC 5-blade FLAIR-2)
- Three-blade carbon-fiber propeller : Carbon hub and full blades (E-PROPS 3-blade A42 22deg)

All tests were performed using a **Lycoming O-360-A1D engine** equipped with a hollow crankshaft. Crankshaft output torque was measured using internal strain gauges.

Measurements were carried out:

- On ground and in flight for most configurations
- On ground only for the FLAIR-2 configuration, as this propeller was decertified by EASA following several mechanical issues. This propeller was nevertheless included in the present study in order to improve understanding of the underlying phenomena that contributed to these issues, with the objective of ensuring that such conditions are not reproduced in future propeller designs.

2. Vibratory Load Analysis Method

Crankshaft vibratory torque data were processed using a **rainflow cycle counting technique**, in accordance with established fatigue analysis practices. The rainflow algorithm is a cycle counting method used to identify and quantify stress or load cycles within a complex, variable-amplitude time history by decomposing the signal into equivalent cyclic load ranges and mean values.

The measured torque time histories were divided into consecutive one-second intervals, each corresponding to a quasi-steady engine operating condition. For each one-second interval, a rainflow analysis was performed to extract torque cycles and their associated ranges.

To focus on sustained vibratory excitation relevant to fatigue damage, only cycle ranges occurring at a rate of at least 20 cycles per second were considered. For each engine speed (RPM), the maximum torque range meeting this occurrence criterion within the corresponding one-second interval was selected and assigned to that RPM.

The minimum cycle frequency threshold of 20 Hz was selected in order to remain below the first engine harmonic frequency for engine speeds above approximately 1200 RPM, ensuring that all relevant torsional excitation phenomena are captured.

This methodology provides a conservative envelope of high-frequency vibratory torque loading as a function of engine speed, while excluding isolated or transient events that are not representative of continuous vibratory excitation.

3. Instrumentation and Measurement System

Crankshaft torque measurements were performed using two full Wheatstone bridge strain-gauge assemblies bonded to the crankshaft at ±45° relative to the shaft axis, a configuration selected to maximize sensitivity to torsional strain while minimizing the influence of bending and axial loads. The strain gauges were installed at a distance of 30 mm from the engine flange face (Figure 1), ensuring measurement of torque in a region representative of the load transmitted to the propeller.

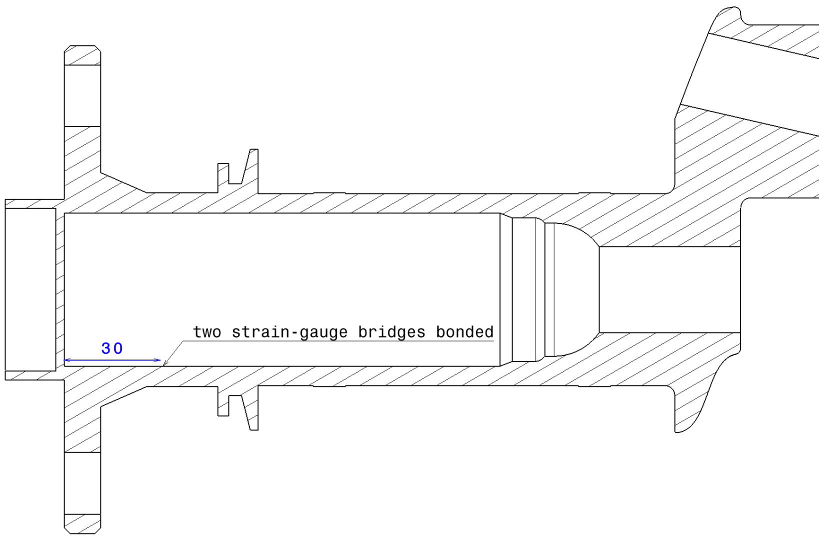

Figure 1: Position of the strain-gauge Wheatstone bridge.

All tests were conducted using the same strain-gauge bridges and identical measurement electronics, ensuring consistency and traceability across the entire test campaign.

The measurement chain was calibrated prior to testing using a static torque calibration procedure performed on a separate, disassembled crankshaft. This reference crankshaft was of the same model and instrumented with identical strain gauges installed at the same locations and orientations as those used for the flight and ground tests. Calibration stability was verified over the duration of the measurement campaign, and no significant drift was observed.

Table 1: Data Acquisition System Specifications

Parameter	**Value**
Acquisition system	E-PROPS ELIAS
Number of channels	16 channels
Sampling rate	6.5 kHz per channel
Synchronization	Aircraft sensors (GPS, altitude, etc.)
Data transmission	Real-time (Wi-Fi + 3G)

Data acquisition was performed using the E-PROPS ELIAS system, comprising a 16-channel acquisition unit operating at a sampling rate of 6.5 kHz per channel. Torque measurements were time-synchronized with the aircraft's other onboard sensors (engine parameters, GPS, altitude, etc.), enabling precise correlation between vibratory torque levels and operating conditions.

Measurement data were transmitted in real time via Wi-Fi and 3G links to both the pilot and the ground test engineer, allowing continuous supervision of data integrity and test execution.

For reasons related to industrial confidentiality, the absolute values and exact frequency levels of the measured vibratory torque data are not disclosed. Results are therefore presented in a comparative and normalized form, preserving the relevance of the analysis.

4. Background and Analysis Framework

4.1 The LUKY Software

The LUKY software is an in-house propeller design and optimization tool developed to model the dynamic interaction between the engine and the propeller. The software incorporates a coupled engine–propeller torsional dynamic model, enabling prediction of vibratory torque transmission across the operating speed range.

Based on this dynamic model, LUKY implements evolutionary optimization algorithms to explore the design space of blade geometry, mass distribution, and aerodynamic parameters, with the objective of reducing vibratory coupling and minimizing torsional excitation amplitudes while preserving aerodynamic performance.

Dynamic simulations performed within LUKY also predict large-amplitude blade-tip motions in specific vibratory operating ranges, providing insight into the structural response of the propeller under resonance conditions. This capability allows potential resonance phenomena to be identified and mitigated early in the design phase, contributing to improved vibratory behavior of the final propeller configuration without reliance on post-design tuning.

4.2 Torsional Resonances

Torsional resonances in engine–propeller systems are characterized by significant amplification of cyclic torque and associated stress levels. When operating near a torsional resonance, the resulting high-amplitude alternating loads can substantially accelerate fatigue damage accumulation in the crankshaft, propeller hub, and blades, potentially leading to premature cracking or structural failure.

At operating points where maximum oscillatory torque is observed in the crankshaft, maximum torsional accelerations at the free end of the crankshaft are also reached. This behavior is consistent with the system dynamics, which can be modeled as a mass–spring system in which the rotating masses remain unchanged. In such a system, alternating inertial forces arise from mass accelerations, resulting in periodic energy transfer between kinetic energy and elastic energy stored in the torsional stiffness of the drivetrain.

Consequently, large torque oscillations transmitted to the propeller are directly associated with high crankshaft accelerations at its free end, generating significant dynamic forces on engine accessories, notably magnetos. This confirms that propeller inertia alone does not protect engine accessories from such dynamic loading.

For these reasons, continuous operation within identified torsional resonance speed ranges should be strictly avoided, and engine–propeller combinations must be designed and operated to either shift resonance frequencies outside the normal operating envelope or minimize excitation levels within these critical regimes.

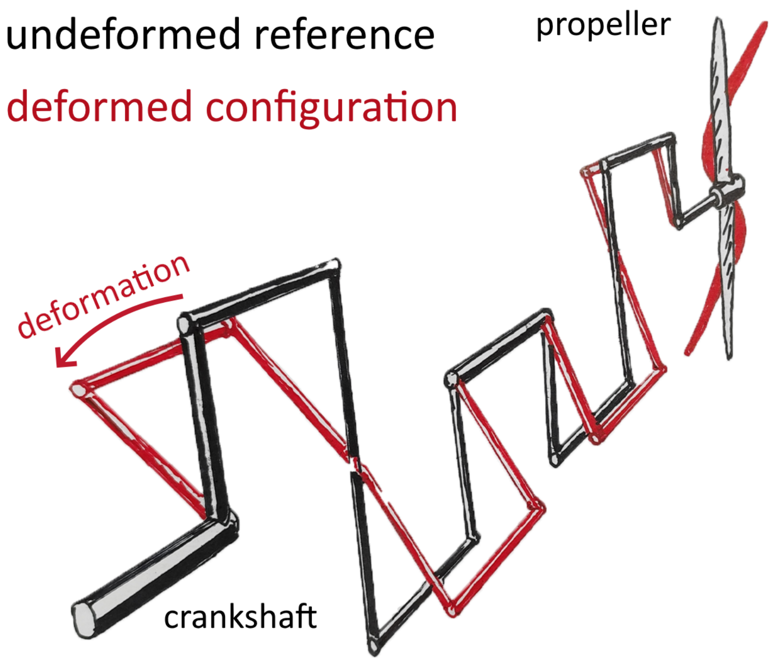

Figure 2: Torsional mode shape of the crankshaft–propeller assembly.

Figure 2 illustrates a torsional mode shape of the crankshaft–propeller assembly, comparing the undeformed reference configuration with the corresponding deformed shape. The mode is characterized by large torsional deformation amplitudes and a single nodal point located within the propeller, indicating strong dynamic coupling between the crankshaft and propeller blades.

For such mode shapes, the static mass moment of inertia of the propeller does not adequately characterize its dynamic behavior, as the vibratory response is governed by the distributed mass, stiffness, and mode shape of the assembly rather than by a single lumped inertia parameter.

5. Data Representation

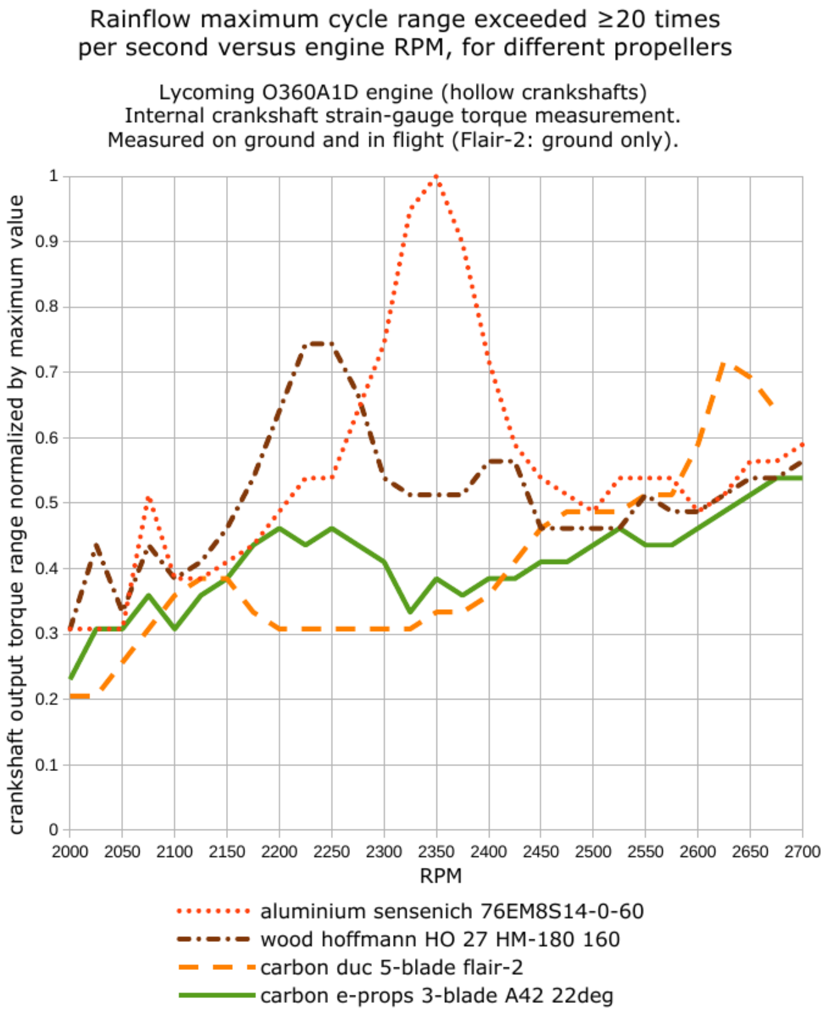

Figure 3: Torsional vibratory torque amplitude as a function of engine speed for different propeller configurations.

6. Results and Discussion

6.1 Aluminium Propeller

The aluminium propeller exhibits a strong vibratory resonance centered around 2350 RPM. The manufacturer's restricted operating range for this propeller is specified between 2150 and 2350 RPM, indicating that the resonance frequency appears to have shifted upward.

Possible contributing factors include:

- Manufacturing tolerances of both the propeller and the engine.
- Reduction of blade mass due to repair or rework operations.

It is considered unlikely that the blade stress peak occurs at a significantly lower frequency than the corresponding crankshaft stress peak. It should be noted that the service bulletin prohibiting continuous operation in this RPM range dates back to 1969.

6.2 Wooden Propeller

The wooden propeller shows a resonance around 2225 RPM, with a moderate vibratory torque level when compared to the aluminium propeller. Although wooden propellers are generally known for their good damping characteristics, this does not eliminate the risk associated with an unfavorably positioned resonance, for example within the cruise RPM range. Even if well tolerated by the propeller itself, such a resonance may still adversely affect the engine and associated components due to sustained torsional excitation.

In this context, it is noteworthy that the operating speed range around 2225 RPM is not identified as a range to be avoided during cruise operation, particularly considering the potential implications for engine accessories subjected to sustained torsional loading.

6.3 Five-Blade Carbon-Fiber Propeller (FLAIR)

The five-blade carbon-fiber propeller exhibits a resonance near 2625 RPM. This propeller was tested with a smaller blade pitch than the nominal flight pitch, allowing the engine to reach 2700 RPM on the ground at zero airspeed.

Increasing blade pitch for flight operation generally tends to reduce the resonance frequency, suggesting that vibratory behavior may be more severe under flight conditions. It also appears possible that, on engines equipped with rigid crankshafts, the resonance frequency could be above 2700 RPM. Identification of the exact engine variants (crankshaft configuration and counterweights) affected by this configuration would therefore be of interest.

The observed resonance is associated with significant blade-tip motion, as predicted by the dynamic reproduction of the engine–propeller system within the LUKY simulation framework. Further investigation of the contribution of these motions to the overall acoustic signature would be valuable.

6.4 Three-Blade Carbon-Fiber Propeller (E-PROPS)

The E-PROPS three-blade carbon-fiber propeller shows only a very slight resonance around 2250 RPM, with significantly lower crankshaft torque levels than those observed for the other propellers.

These results demonstrate the effectiveness of the vibratory coupling reduction work performed during the design phase using evolutionary optimization algorithms within the LUKY software, targeting minimization of torsional excitation.

Part of the improvement can also be attributed to the Extended Speed Range (ESR) effect, which reduces the variation of full-throttle engine speed between takeoff and high-speed flight conditions. This allows higher engine speeds during takeoff for a given cruise pitch, improving takeoff performance. From a vibratory standpoint, the narrower full-throttle RPM range reduces the likelihood of operating at resonance under wide-open throttle conditions.

In contrast, traditional wide-blade propellers typically exhibit larger full-throttle RPM variations, making the intersection between structural natural frequencies and engine harmonic excitations nearly unavoidable.

The strong similarity of the measured engine torque levels outside resonance conditions, despite the use of propellers with very different mass moments of inertia—the aluminium propeller exhibiting a moment of inertia several times higher than that of the wooden and carbon-fiber propellers-indicates that, under normal operating conditions, the propeller mass moment of inertia is not a dominant parameter in the steady-state engine-propeller interaction.

7. Conclusion

Among the tested configurations, the E-PROPS carbon-fiber propeller demonstrates the most favorable vibratory behavior, with minimal resonance amplitude and reduced torque excitation. In contrast, aluminium and multi-blade carbon-fiber propellers exhibit pronounced resonances within or near typical operating RPM ranges, with potential implications for durability, comfort, and long-term fatigue behavior.

These results provide a basis for the development of more efficient, quieter, and reliable propeller solutions for direct-drive engine applications. However, verification of resonance RPM ranges for each engine–propeller configuration remains essential, as vibratory behavior is influenced by crankshaft stiffness, piston mass, spacer stiffness, and propeller characteristics.

The presence of a crankshaft equipped with 6.3 and 8th order pendulum counterweights can reduce vibratory amplitudes for targeted harmonic orders, but does not address all resonance conditions. In this context, the high stiffness carbon-fiber spacers used on E-PROPS propellers contribute to limiting additional compliance and stabilizing resonance placement, in combination with overall engine-propeller dynamic optimization.

A. Author Contributions

Jérémie Buiatti: Study leadership, methodology definition, supervision of the experimental campaign, coordination of data analysis, development of the LUKY software, and interpretation of results.

Habib Setti: Development and implementation of the LUKY dynamic engine model, support of the evolutionary optimization framework, and analysis of simulation results in correlation with experimental data.

Himaé Guigne: Lead test engineering, including test definition, instrumentation setup, synchronization of measurement systems, validation of acquired data, and analysis and correlation of experimental results with numerical predictions.

Yoann Cossec: Responsibility for the direct-drive engine propeller product line, design, manufacturing, and assembly of propeller prototypes, definition of test configurations, and alignment of prototype design choices with experimental objectives.

Samuel Dupland: Flight test operations, definition of safe and representative test points, and execution of the flight test program.